

LETTER

Comparative planetary mineralogy: V/(Cr + Al) systematics in chromite as an indicator of relative oxygen fugacity

J.J. PAPIKE,\* J.M. KARNER, AND C.K. SHEARER

Institute of Meteoritics, Department of Earth and Planetary Sciences, University of New Mexico, Albuquerque, New Mexico 87131-1126, U.S.A.

ABSTRACT

We have been developing oxygen barometers based largely on the behavior of V, which can occur in four valence states ( $V^{2+}$ ,  $V^{3+}$ ,  $V^{4+}$ , and  $V^{5+}$ ), and record at least 8 orders of magnitude of  $f_{O_2}$ . Our first efforts in measuring these valence proportions were by XANES techniques in basaltic glasses from Earth, Moon, and Mars. We now address the behavior of V valence states in chromite in basalts from these bodies with a technique that uses the electron microprobe. Our first insights into this new technique resulted from running electron probe traverses across spinel grains from core to rim on grains that show zoning from chromite to ulvöspinel. The zoning profiles showed the normal trends of core to rim decreases of Cr, Al, and Mg, and increases of Fe, Ti, and Mn. However, the behavior of V was very different for Moon and Earth, with Mars in between. In terrestrial basalts  $V^{4+} > V^{3+}$ , in lunar basalts  $V^{3+} > V^{4+}$ , and in martian basalts  $V^{3+}$  and  $V^{4+}$  are both significant. The trends (core to rim) for the Moon show a strong positive correlation of V and Cr and negative correlation of V and Ti. For the Earth, the trends are just the opposite, with a strong negative correlation for V and Cr and a strong positive correlation of V and Ti. Chromite in martian basalts showed trends somewhere in between. We found that a convenient way to display these data for chromite is a plot showing the relative V/(Cr + Al) ratios. These ratios nicely reflect the oxygen fugacity ranges for Moon, Mars, and Earth.

INTRODUCTION

As our part of the new “Oxygen in the Solar System” initiative of the Lunar and Planetary Institute, we have been developing oxybarometers largely based on the behavior of V, which can occur in four valence states ( $V^{2+}$ ,  $V^{3+}$ ,  $V^{4+}$ , and  $V^{5+}$ ) and record at least 8 orders of magnitude variation in oxygen fugacity ( $f_{O_2}$ ) (Sutton et al. 2004). Figure 1 illustrates the relationship between the V valence-state transitions and the valence-state transitions of other selected multivalent cations. Our first efforts in measuring these valence proportions were by X-ray Absorption Near Edge Structure (XANES) techniques in basaltic glasses from Earth, Moon, and Mars (Sutton et al. 2004; Karner et al. 2004a). We now address the behavior of V valence states in chromite in basalts from these bodies. We have been looking for a “V in chromite oxybarometer” that works with data collected by the electron microprobe and thus is readily accessible to a large segment of the planetary materials community. This paper describes our results in this effort.

Previous work recognized the potential of V for estimates of  $f_{O_2}$ . Lindstrom (1976) was the first to report experimental results confirming that the partitioning behavior of V is dependent on  $f_{O_2}$ . Canil (1999) studied V partitioning among orthopyroxene, spinel, and silicate melt and the redox states of mantle source regions for primary magmas. Pearce et al. (2000) used V vs. Yb systematics to assess  $f_{O_2}$  in fore-arc peridotites. Canil and Fedortchouk (2001) addressed olivine – liquid partitioning of V, with applications to modern and ancient picrites. Shervais (1982) used Ti-V plots to understand the petrogenesis of modern and ophiolitic magmas. Canil (2002) studied V in peridotites, mantle redox, and tectonic environments. It is this paper that is most relevant to our present

work because Canil (2002) did partitioning studies of V between several basalt and chromite compositions and showed that for spinel with high Cr/Al, the  $D$ -values for V (spinel/melt) increases dramatically from  $\sim 2$  at high  $f_{O_2}$  [Iron-Wüstite (IW) + 5] to  $\sim 32$  at low  $f_{O_2}$  (IW-2). Connolly and Burnett (2003) studied the  $f_{O_2}$  dependence of  $D$ -values for V and Ti.

Therefore, with this background we initiated the present study, which is a part of our continuing efforts in comparative planetary mineralogy. Two of our recent studies in this area are Karner et al. (2003), on olivine from planetary basalts, and Karner et al. (2004b) on plagioclase from planetary basalts. Thus this paper, on chromite from planetary basalts, will be the third in this series. The sample suites we used for this study are described in Table 1.

ANALYTICAL TECHNIQUES

Chromite grains in thin sections from 11 samples (see Table 1) were analyzed to determine their major- and minor-element compositions. Samples were selected that contained chromite as an early liquidus phase. Analyses were made at the University of New Mexico’s microbeam facilities using a JEOL JXA 8200 microprobe equipped with a back-scattered electron detector, a thin-window energy dispersive spectrometer, and five wavelength-dispersive spectrometers. Chromite analyses were made using an accelerating voltage of 15 kV, a beam current of 20 nA, and a beam diameter of 1  $\mu$ m. The analytical routine included calibration of Si on olivine, Ti on rutile, Mg, Al, and Cr on chromite, Mn on spessartine, Fe on pure Fe metal, and V on pure V metal. All the standards were from the C.M. Taylor Corporation. Wavelength dispersive spectrometer counting times were as follows: 20 s on peak and 10 s on backgrounds for Si, Al, Cr, Fe, and Mg; 30 s on peak and 15 s on backgrounds for Ti; and 40 s on peak and 20 s on backgrounds for V and Mn. Vanadium concentrations were corrected for interference from the  $TiK\alpha$  peak by the procedure described in Snetsinger et al. (1968), and resulted in  $\sim 6\%$  of the total Ti counts being subtracted from the total V counts. Likewise, Mn was corrected for interference from the  $CrK\alpha$  peak, and resulted in  $\sim 0.1\%$  of the total Cr counts being subtracted from the total Mn counts. All data were reduced using a ZAF correction program and cast as oxide wt% with Fe as FeO, Cr as  $Cr_2O_3$ , and V as  $V_2O_3$ .

\* E-mail: jpapike@unm.edu

RESULTS

For a review of spinel crystal chemistry refer to Papike et al. (1976), Wechsler et al. (1984), and Waychunas (1991), and important crystal chemical details of solid solution between

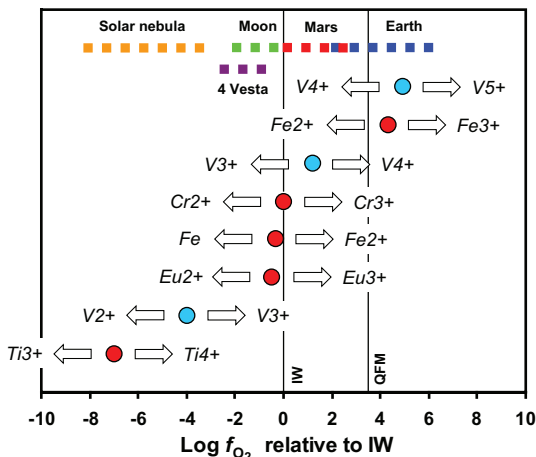


FIGURE 1. Schematic diagram of variable-valence elements plotted at the  $f_{O_2}$  (relative to the IW buffer) where they occur. The circles represent the point (in  $\log f_{O_2}$ ) at which the oxidized and reduced species of an element exist in equal proportions in a basaltic melt. Note the great range over which V valences occur, covering over 8 orders of magnitude and spanning the  $f_{O_2}$  range of the solar system. The data used to construct this diagram are from Schreiber (1987) for Eu; Schreiber et al. (1987) for Fe; Hanson and Jones (1998) for Cr; Beckett (1986) for Ti; and Karner et al. (2004a), Sutton et al. (2002), and Canil (1999) for V.

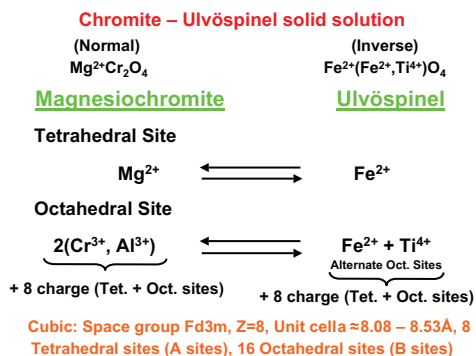


FIGURE 2. Crystal-chemical aspects of solid solution between chromite and ulvöspinel.

chromite and ulvöspinel are illustrated in Figure 2. Our first insights into this technique resulted from performing electron probe traverses across spinel grains, analyzing for Cr, Al, Ti, Fe, Mg, Mn, and V from core to rim on grains that show zoning from chromite to ulvöspinel. Representative electron microprobe analyses are reported in Table 2, and two typical zoning profiles are illustrated in Figure 3. Figure 3a is for a chromite from a Hawaiian basalt and Figure 3b is for a chromite from a lunar basalt. The zoning profiles of all spinel grains studied show the normal trends of core to rim decreases of Cr, Al, and Mg, and increases of Fe, Ti, and Mn. However, much to our surprise and delight, the V behavior was very different for the Moon and

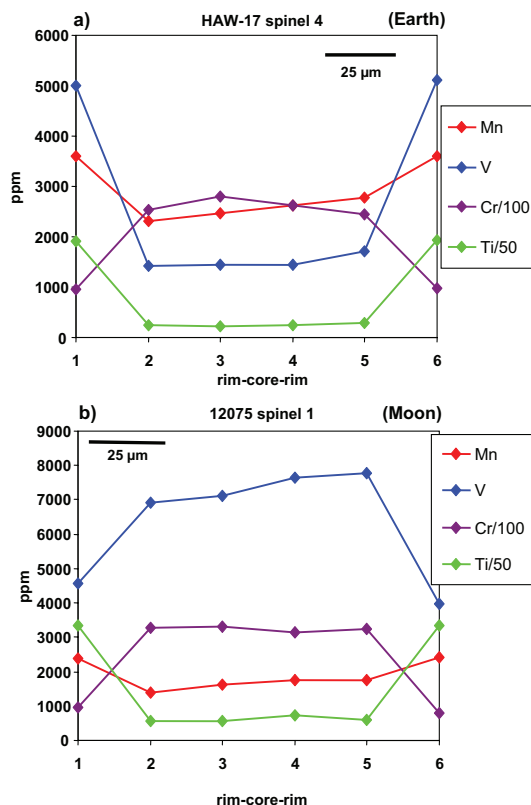


FIGURE 3. Typical zoning profiles for a terrestrial spinel grain from a Hawaiian (HAW-17) basalt (Fig. 3a), and for a spinel from lunar basalt 12075 (Fig. 3b). Traverses were done on grains zoned from chromite cores to Fe-Ti spinel rims, with approximately 25 µm steps.

TABLE 1. Basalt suites chosen for chromite analysis in this study, along with corresponding setting, locality, thin section number, and rock type.

| Sample suite               | Geological/Tectonic setting                               | Locality  | Thin section-rock type  | Reference  |
|----------------------------|---|---|---|--|
| Ocean floor basalts        | Mid-ocean ridge, divergent plate volcanism                | Mid-Atlantic Ridge  | OF-3 Primitive basalt   | Rhodes et al. 1981   |
| Island Arc basalts         | Volcanism onto ocean floor at convergent plate boundaries | New Britain, Papua-New Guinea                             | IA-11 Vesicular basalt  | Taylor et al. 1981   |
| Oceanic Intraplate basalts | Oceanic-island hotspot volcanism                          | Hawaiian islands, U.S.A.<br>Kilauea Iki-1<br>Makaopuhi-22 | HAW-17 Ankaramite<br>Olivine tholeiite<br>Olivine tholeiite                         | Bence 1981<br>Shearer (Unpublished)<br>Wright and Okamura 1965 |
| Lunar Basalts              | Lunar mare basaltic volcanism                             | Apollo 12 and 15 landing sites                            | 12020, 12075 AP12<br>Olivine basalts; 12063<br>AP12 Ilmenite basalt;                | Papike et al. 1976   |
| Martian Basalts            | Martian basaltic volcanism                                | Meteorites-Dar al Gani 476,<br>EETA 79001                 | 15595 AP15 Pigeonite basalt<br>Dar al Gani 476, EETA<br>79001 Basaltic shergottites | Meyer 1998   |

**TABLE 2.** Average composition of chromite (core), and a representative Fe-Ti spinel composition (rim) in grains from planetary basalts

| Sample                         | Hawaii-17 | Ocean Kilauea     | Makaopuhi     | Island           | EETA 79001 | Dar al Gani 476 | 12075  | 12020  | 12063  | 15595  |        |        |        |        |        |        |        |
|--------------------------------|-----------|-------------------|---------------|------------------|------------|-----------------|--------|--------|--------|--------|--------|--------|--------|--------|--------|--------|--------|
|                                | N = 9     | Floor-3<br>N = 11 | Iki<br>N = 11 | Arc-11<br>N = 10 | N = 13     | N = 6           | N = 11 | N = 10 | N = 9  | N = 16 |        |        |        |        |        |        |        |
|                                | core      | rim               | core          | core             | core       | rim             | core   | rim    | core   | rim    |        |        |        |        |        |        |        |
| SiO <sub>2</sub> (wt%)         | <0.04     | <0.04             | 0.04          | <0.04            | <0.04      | <0.04           | 0.08   | <0.04  | <0.04  | 0.06   | <0.04  | 0.05   | <0.04  | 0.06   | <0.04  |        |        |
| Al <sub>2</sub> O <sub>3</sub> | 15.36     | 7.72              | 28.64         | 14.06            | 14.32      | 26.84           | 7.19   | 5.41   | 7.75   | 6.41   | 12.74  | 3.37   | 12.28  | 4.10   | 11.62  | 4.73   | 12.15  |
| TiO <sub>2</sub>               | 2.15      | 12.45             | 0.41          | 2.34             | 2.92       | 0.91            | 0.77   | 11.92  | 1.20   | 17.49  | 4.58   | 27.85  | 4.27   | 25.74  | 7.98   | 25.90  | 2.58   |
| Cr <sub>2</sub> O <sub>3</sub> | 41.69     | 26.64             | 36.77         | 43.73            | 38.87      | 34.36           | 58.20  | 35.43  | 58.64  | 29.62  | 48.53  | 13.97  | 49.12  | 16.40  | 42.63  | 16.67  | 52.55  |
| MgO                            | 7.82      | 6.24              | 16.06         | 10.84            | 11.03      | 13.30           | 3.23   | 2.76   | 4.04   | 4.22   | 6.30   | 1.33   | 5.02   | 1.54   | 2.76   | 1.56   | 7.27   |
| FeO                            | 32.91     | 44.54             | 18.36         | 28.48            | 31.71      | 24.59           | 30.50  | 42.88  | 28.84  | 42.31  | 27.90  | 53.56  | 29.74  | 51.95  | 36.03  | 51.90  | 25.32  |
| MnO                            | 0.29      | 0.32              | 0.17          | 0.21             | 0.22       | 0.21            | 0.41   | 0.46   | 0.43   | 0.52   | 0.21   | 0.31   | 0.21   | 0.24   | 0.23   | 0.26   | 0.22   |
| V <sub>2</sub> O <sub>3</sub>  | 0.23      | 0.65              | 0.20          | 0.26             | 0.28       | 0.23            | 0.58   | 0.85   | 0.75   | 0.74   | 1.04   | 0.67   | 0.97   | 0.68   | 0.93   | 0.84   | 1.02   |
| Total                          | 100.45    | 98.56             | 100.66        | 99.96            | 99.36      | 100.45          | 100.91 | 99.80  | 101.69 | 101.32 | 101.32 | 101.12 | 101.62 | 100.69 | 102.21 | 101.90 | 101.11 |

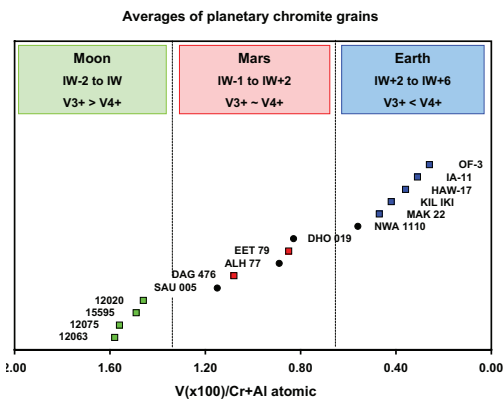
  

| Formula proportions of cations based on 4 O atoms |      |      |      |      |      |      |      |      |      |      |      |      |      |      |      |      |      |
|---|------|------|------|------|------|------|------|------|------|------|------|------|------|------|------|------|------|
| Si  | 0.00 | 0.00 | 0.00 | 0.00 | 0.00 | 0.00 | 0.00 | 0.00 | 0.00 | 0.00 | 0.00 | 0.00 | 0.00 | 0.00 | 0.00 | 0.00 | 0.00 |
| Al  | 0.61 | 0.33 | 1.00 | 0.55 | 0.57 | 0.97 | 0.30 | 0.23 | 0.31 | 0.26 | 0.50 | 0.14 | 0.48 | 0.17 | 0.46 | 0.20 | 0.47 |
| Ti  | 0.05 | 0.34 | 0.01 | 0.06 | 0.07 | 0.02 | 0.02 | 0.32 | 0.03 | 0.45 | 0.11 | 0.75 | 0.11 | 0.69 | 0.20 | 0.68 | 0.06 |
| Cr  | 1.10 | 0.76 | 0.86 | 1.14 | 1.03 | 0.83 | 1.61 | 1.01 | 1.59 | 0.81 | 1.27 | 0.39 | 1.29 | 0.46 | 1.14 | 0.46 | 1.37 |
| Mg  | 0.39 | 0.33 | 0.71 | 0.54 | 0.55 | 0.61 | 0.17 | 0.15 | 0.21 | 0.22 | 0.31 | 0.07 | 0.25 | 0.08 | 0.14 | 0.08 | 0.36 |
| Fe  | 0.92 | 1.34 | 0.46 | 0.79 | 0.89 | 0.63 | 0.89 | 1.29 | 0.83 | 1.22 | 0.77 | 1.59 | 0.83 | 1.55 | 1.02 | 1.52 | 0.70 |
| Mn  | 0.01 | 0.01 | 0.00 | 0.01 | 0.01 | 0.01 | 0.01 | 0.01 | 0.01 | 0.02 | 0.01 | 0.01 | 0.01 | 0.01 | 0.01 | 0.01 | 0.01 |
| V   | 0.01 | 0.02 | 0.00 | 0.01 | 0.01 | 0.01 | 0.02 | 0.02 | 0.02 | 0.02 | 0.03 | 0.02 | 0.03 | 0.02 | 0.03 | 0.02 | 0.03 |
| Total*  | 3.09 | 3.11 | 3.05 | 3.09 | 3.12 | 3.07 | 3.02 | 3.04 | 3.00 | 3.00 | 2.99 | 2.98 | 2.99 | 2.98 | 2.99 | 2.98 | 3.00 |

\* High cation sums, relative to 3.00, are likely the result of Fe<sup>3+</sup>, especially in terrestrial spinel grains.

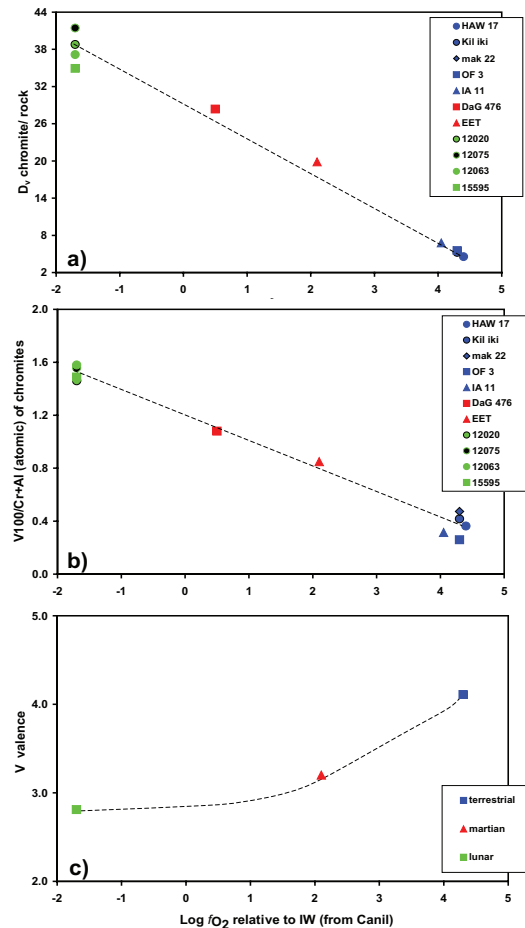
Earth. In terrestrial basalts V<sup>4+</sup> > V<sup>3+</sup>, in lunar basalts V<sup>3+</sup> > V<sup>4+</sup>, and in martian basalts V<sup>3+</sup> and V<sup>4+</sup> are both significant (Karner et al. 2004a). The trends (core to rim) for the lunar spinel show a strong positive correlation of V and Cr and a negative correlation of V and Ti. In terrestrial spinel, the trends are just the opposite, with strong negative correlation for V and Cr and a strong positive correlation of V and Ti. Chromite in martian basalts showed

trends somewhere in between, with DaG 476 showing lunar-type trends and EETA 79001 (lithology A) showing terrestrial-type trends. According to Wadhwa (2001) and Herd et al. (2002), EETA 79001 (lithology A) crystallized at a higher f<sub>o2</sub> than DaG



**FIGURE 4.** Average V × 100/(Cr + Al) (atomic) ratios for chromite grains from planetary basalts. Also shown are the f<sub>o2</sub> ranges estimated for materials from Earth, Moon, and Mars, along with the relative proportions of V<sup>3+</sup> and V<sup>4+</sup> in these bodies. The squares are data from this study, whereas the dots are data from Goodrich et al. (2003).

**FIGURE 5.** Stacked diagram showing the relationships of D<sub>v</sub> chromite/rock, V × 100/(Cr + Al) (atomic) of chromite, and V valence with log f<sub>o2</sub> relative to IW, for planetary basalts. In Figure 5a, D<sub>v</sub> was determined by using our measured V in chromite with literature values of V in the rock; log f<sub>o2</sub> values (X-axis) were calculated from Canil (2002). Figure 5b is a plot of our ratio V(x 100)/(Cr + Al) plotted in the same way. Figure 5c is derived from the work described in Sutton et al. (2004) and Karner et al. (2004). All trend lines are approximate.



476. We found that a convenient way to display these data for chromite cores is a plot showing the relative  $V/(Cr + Al)$  ratios (Fig. 4). Because  $D_V$  increases with decreasing  $f_{O_2}$ , the trend of these ratios nicely differentiate the  $f_{O_2}$  ranges for Earth, Moon, and Mars. Thus, it appears that these simple measurements, using only an electron microprobe on single chromite grains, can yield significant qualitative data about planetary parentage and relative  $f_{O_2}$ . This technique would be particularly useful for isolated chromite grains from a planetary regolith, which will probably be the main type of sample returned from future planetary missions.

Of course, much more quantitative estimates of  $f_{O_2}$  can be made when we have a basalt that represents a melt (not a cumulate) with chromite that is in equilibrium with the melt. Such rocks are not easy to find in planetary environments where our sample suite is small. For example, both martian rocks used in this study are cumulates, not melts, which is why we use the term mineral/rock rather than mineral/melt. Nevertheless, we have tried to move this new chromite technique one step further, as illustrated in Figure 5. Figure 5a was enabled by the work of Canil (2002) who reported  $D_V$  chromite/liquid over a range of  $f_{O_2}$  values from IW+5 to IW-2. We used our measured  $V$  in chromite with literature values of  $V$  in the rock (usually not a melt) and  $D$  values of Canil to make this diagram. The  $\log f_{O_2}$  values on the X-axis are from Canil (2002). Figure 5b is a plot of our ratio  $V(\times 100)/(Cr + Al)$  plotted in the same way. Figure 5c is derived from the work described in Sutton et al. (2004) and Karner et al. (2004a).

In summary, we have presented a simple technique that uses only electron microprobe data from single chromite grains that yields much information on planetary parentage and relative oxygen fugacity.

#### ACKNOWLEDGMENTS

This research was supported by a NASA Cosmochemistry Grant to JJP. We thank Mike Spilde for significant help with the EMP strategy, especially with correcting for the Ti-V interference. We are grateful for the constructive reviews of Steve Simon, John Shervais, and Bob Dymek.

#### REFERENCES CITED

- Bence, A.E. (1981) Oceanic intraplate volcanism. In R.B. Merrill and R. Ridings, Eds., *Basaltic Volcanism on the Terrestrial Planets*, p. 161–192. Pergamon, New York.
- Beckett, J.R. (1986) The origin of calcium-, aluminum-rich inclusions from carbonaceous chondrites: an experimental study. Ph.D. thesis, University of Chicago.
- Canil, D. (1999) Vanadium partitioning between orthopyroxene, spinel, and silicate melt and the redox states of mantle source regions for primary magmas. *Geochimica et Cosmochimica Acta*, 63, 557–572.
- (2002) Vanadium in peridotites, mantle redox state and tectonic environments: Archean to present. *Earth and Planetary Science Letters*, 195, 75–90.
- Canil, D. and Fedortchouk, Y. (2001) Olivine-liquid partitioning of vanadium and other trace elements, with applications to modern and ancient picrites. *The Canadian Mineralogist*, 39, 319–330.
- Connolly, H.C. and Burnett, D.S. (2003) On type B CAI formation: experimental constraints on  $f_{O_2}$  variations in spinel minor element partitioning and re-equilibration effects. *Geochimica et Cosmochimica Acta*, 63, 557–572.
- Goodrich, C.A., Herd, C.D.K., and Taylor, L.A. (2003) Spinel and oxygen fugacity in olivine-phyric and lherzolitic shergottites. *Meteoritics and Planetary Science*, 38, 1773–1792.
- Hanson, B. and Jones, J.H. (1998) The systematics of  $Cr^{3+}$  and  $Cr^{2+}$  partitioning between olivine and liquid in the presence of spinel. *American Mineralogist*, 83, 669–684.
- Herd, C.D.K., Borg, L.E., Jones, J.H., and Papike, J.J. (2002) Oxygen fugacity and geochemical variations in the martian basalts: implications for martian basalt petrogenesis and the oxidation state of the upper mantle of Mars. *Geochimica et Cosmochimica Acta*, 66, 2025–2036.
- Karner, J.M., Papike, J.J., and Shearer, C.K. (2003) Olivine from planetary basalts: Chemical signatures that indicate planetary parentage and those that record igneous setting and process. *American Mineralogist*, 88, 806–816.
- Karner, J.M., Sutton, S.R., Papike, J.J., Delaney, J.S., Shearer, C.K., Newville, M., Eng, P., Rivers, M., and Dyar, M.D. (2004a) A new oxygen barometer for solar system basaltic glasses based on vanadium valence (abstract). Lunar and Planetary Science Conference XXXV no. 1269. Lunar and Planetary Institute, Houston, (CD-ROM).
- Karner, J.M., Papike, J.J., and Shearer, C.K. (2004b) Plagioclase from planetary basalts: Chemical signatures that reflect planetary volatile budgets, oxygen fugacity, and styles of igneous differentiation. *American Mineralogist*, 89, 1101–1109.
- Lindstrom, D.J. (1976) Experimental study of partitioning of the transition metals between clinopyroxene and coexisting silicate liquids. Ph.D. thesis, University of Oregon.
- Meyer, C. (1998) Mars Meteorite Compendium-1998. JSC no. 27672, 237 p. NASA Johnson Space Center, Houston. See <http://www.curator.jsc.nasa.gov/curator/antmet/mmc/mmc.htm> for updates.
- Papike, J.J., Hodges, F.N., Bence, A.E., Cameron, M., and Rhodes, J.M. (1976) Mare basalts: crystal chemistry, mineralogy, and petrology. *Reviews of Geophysics and Space Physics*, 14, 475–540.
- Pearce, J.A., Barker, P.F., Edwards, S.J., Parkinson, I.J., and Leat, P.T. (2000) Geochemistry and tectonic significance of peridotites from South Sandwich arc-basin, South Atlantic. *Contributions to Mineralogy and Petrology*, 139, 36–53.
- Rhodes, J.M. and Bence, A.E. (1981) Ocean floor basaltic volcanism. In R.B. Merrill and R. Ridings, Eds., *Basaltic Volcanism on the Terrestrial Planets*, p. 132–160. Pergamon, New York.
- Schreiber, H.D. (1987) An electrochemical series of redox couples in silicate melts: a review and applications to geochemistry. *Journal of Geophysical Research*, 92, 9225–9232.
- Schreiber, H.D., Merkel, R.C., Schreiber, V.L., and Balazs, G.B. (1987) Mutual interactions of redox couples via electron exchange in silicate melts: models for geochemical melt systems. *Journal of Geophysical Research*, 92, 9233–9245.
- Shervais, J.W. (1982) Ti-V plots and the petrogenesis of modern and ophiolitic lavas. *Earth and Planetary Science Letters*, 59, 101–118.
- Snetsinger, K.G., Bunch, T.E., and Keil, K. (1968) Electron microprobe analysis of vanadium in the presence of titanium. *American Mineralogist*, 53, 1770–1773.
- Sutton, S.R., Simon, S.B., Grossman, L., Delaney, J.S., Beckett, J., Newville, M., Eng, P., and Rivers, M. (2002) Evidence for divalent vanadium in Allende CAI fassaite and implications for formation conditions (abstract). Lunar and Planetary Science Conference XXXIII no. 1907. Lunar and Planetary Institute, Houston, (CD-ROM).
- Sutton, S.R., Karner, J.M., Papike, J.J., Delaney, J.S., Shearer, C.K., Newville, M., Eng, P., Rivers, M., and Dyar, D.M. (2004) Oxygen barometry of basaltic glasses based on vanadium valence determinations using synchrotron microXANES (abstract). Lunar and Planetary Science Conference XXXV no. 1725. Lunar and Planetary Institute, Houston, (CD-ROM).
- Taylor, S.R., Arculus, R., Perfit, M.R., and Johnson, R.W. (1981) Island arc basalts. In R.B. Merrill and R. Ridings, Eds., *Basaltic Volcanism on the Terrestrial Planets*, p. 193–213. Pergamon, New York.
- Wadhwa, M. (2001) Redox state of Mars' upper mantle and crust from Eu anomalies in shergottite pyroxenes. *Science*, 291, 1527–1530.
- Waychunas, G.A. (1991) Crystal chemistry of oxides and oxyhydroxides. In D.H. Lindsley, Ed., *Oxide minerals: petrologic and magnetic significance*, vol. 25, p. 11–68. *Reviews in Mineralogy*, Mineralogical Society of America, Washington D.C.
- Wechsler, B.A., Lindsley, D.H., and Prewitt, C.T. (1984) Crystal structure and cation distribution in titanomagnetites ( $Fe_{3-x}Ti_xO_4$ ). *American Mineralogist*, 69, 754–770.
- Wright, T.L. and Okamura, R.T. (1977) Cooling and crystallization of tholeiitic basalt, 1965 Makaopuhi Lava Lake, Hawaii, Geological Survey Professional Paper 1004, 78 p. U.S. Government Printing Office, Washington, D.C.

MANUSCRIPT RECEIVED MAY 28, 2004

MANUSCRIPT ACCEPTED JULY 18, 2004

MANUSCRIPT HANDLED BY ROBERT F. DYMEK